TodyComm: Task-Oriented Dynamic Communication for Multi-Round LLM-based Multi-Agent System

Wenzhe Fan [1] **Tommaso Tognoli** [1] **Henry Peng Zou** [1] **Chunyu Miao** [1] **Yibo Wang** [1] **Xinhua Zhang** [1]

Abstract

Multi-round LLM-based multi-agent systems rely on effective communication structures to support collaboration across rounds. However, most existing methods employ a fixed communication topology during inference, which falls short in many realistic applications where the agents' roles may change *across rounds* due to dynamic adversary, task progression, or time-varying constraints such as communication bandwidth. In this paper, we propose addressing this issue through Tody-Comm, a **t**ask-**o**riented **dy**namic **comm**unication algorithm. It produces behavior-driven collaboration topologies that adapt to the dynamics at each round, optimizing the utility for the task through policy gradient. Experiments on five benchmarks demonstrate that under both dynamic adversary and communications budgets, TodyComm delivers superior task effectiveness while retaining token efficiency and scalability.

1. Introduction

Large language model (LLM)-based multi-agent systems (MAS) (Li et al., 2023; Hong et al., 2023; Zhuge et al., 2024; Wu et al., 2024; Liang et al., 2024; Zou et al., 2025) have emerged as a powerful paradigm for collaborative problem solving. Within this research area, multi-agent, multi-round collaboration (Du et al., 2023; Liu et al., 2024) constitutes an important interaction mechanism, in which agents iteratively exchange information across multiple rounds and refine their responses before producing a final solution. Such iterative collaboration enables the integration of diverse reasoning perspectives, supports error correction over time, and progressively improves solution quality, making it particularly effective for complex reasoning, planning, and decision-making tasks (Zhang et al., 2025a; Parmar et al., 2025; Fan et al., 2025; Zhao et al., 2025).

[1]Department of Compute Science, University of Illinois at Chicago, IL, USA. Correspondence to: Wenzhe Fan <wfan23@uic.edu>, Xinhua Zhang <zhangx@uic.edu>.

Recent research on multi-round LLM-based multi-agent systems (MAS) has explored a range of methods for enabling effective collaboration across multiple rounds of interaction. A prominent line of work focuses on communication topology design, where agent interactions are modeled as graphs that are either predefined or optimized to improve collaboration (Zhang et al., 2025a;b;c; Wang et al., 2025b; Li et al., 2025). However, these approaches rely on fixed communication graphs *at inference time*, which prevents adaptation to evolving agent behaviors (e.g., historical response, neighboring info and agent-related info, etc) and consequently degrades the task performance, particularly in dynamic settings.

Complementary to topology design, a growing body of work has investigated the security and robustness of multi-round LLM-based MAS. Existing approaches (Wang et al., 2025a; Miao et al., 2025) primarily rely on graph-based anomaly detection, while Zhou et al. (2026) proposes resilient MAS architectures that tolerate agent corruption. However, Zhou et al. (2026) still depends on a fixed communication graph, and Wang et al. (2025a) and (Miao et al., 2025) do not incorporate task-level feedback (e.g., utility or task accuracy), which can lead to less effective interactions. Moreover, Wang et al. (2025a) requires adversary labels during training, which is impractical in real-world settings.

In this paper, we are motivated by scenarios of LLM-based MAS where the agents' communication graph needs to be adapted *across rounds*. For example, a task must be accomplished through multiple stages, each of which may require a distinct graph. The communication channels may impose time-varying constraints on bandwidth. In a dynamically adversarial setting, agents may randomly transition to adversarial behavior at unknown rounds, while retaining their original roles and producing plausibly structured but misleading analyses to other agents. It reflects realistic collaborative scenarios, where participants may gradually become unreliable due to misunderstanding, bias, fatigue, or external incentives, rather than through explicit role changes.

Despite its importance, learning dynamic communication structures in multi-agent, multi-round settings remains challenging. Directly optimizing discrete inter-agent graphs across rounds induces a combinatorial action space. More-

Table 1. Comparing and contrasting our method with baseline methods. ∗: "Edge selection per round" indicates that graph structures vary across rounds due to changes in the underlying graph distribution, rather than stochastic sampling from an *invariant* set of edge weights. ∗∗: "Edge selection per round in training" means the algorithm changes the edges during training, which in turn **actively impacts the training data**. "-" denotes the absence of adversarial setting in the experiment.

	Edge selection **per round**∗ in **inference**	Edge selection **per round**∗ in **training**∗∗	Node dropout in communication graph	Adversary label **not** required	Parametric edge selector based on agent behavior	Task-driven edge selection	Optimization mode
G-Designer	✗	✗	✗	✓	✗	✓	RL + aux. loss
AgentPrune	✗	✗	✗	✓	✗	✓	RL + aux. loss
AgentDropout	✗	✓	✓	-	✗	✓	RL + aux. loss
SafeSieve	✗	✗	✓	✓	✗	✓	Heuristic
AGP	✗	✗	✓	-	✗	✓	Supervised
G-safeguard	✓	✗	✗	✗	✓	✗	Supervised
BlindGuard	✓	✗	✗	✓	✓	✗	Unsupervised
ResMAS	✗	✗	✗	✓	✓	✓	SFT + GRPO
TodyComm (ours)	✓	✓	✓	✓	✓	✓	RL

over, determining how communication structures should evolve based on agents' behaviors in previous rounds is itself non-trivial, as agent outputs are unstructured, stochastic, and context-dependent.

To address these challenges, we propose TodyComm, a **t**ask-**o**riented framework that **dy**namically learns behavior-driven **comm**unication structures to coordinate LLM-based agents across multiple interaction rounds both in the training and inference. TodyComm models multi-round agent interactions using two graph structures: an inter-agent communication graph for information exchange at each round and a decision graph for final aggregation. The multi-agent, multi-round interaction is formulated as a Markov decision process (Puterman, 1990), where each episode corresponds to solving a query over T interaction rounds, and actions correspond to the trajectories of inter-agent communication graphs across rounds together with the final decision graph.

Inspired by credit assignment in multi-agent reinforcement learning, TodyComm learns agent-level credit values that reflect each agent's contribution and reliability based on historical behaviors and interaction context. These credits are updated using a gated recurrent network (GRN, Chung et al., 2014), enabling the model to capture temporal dependencies across rounds. Graph-level actions are then instantiated as agent participation decisions based on the learned credits, followed by deterministic communication graph construction. This design both simplifies policy learning and naturally extends to node-wise incoming and outgoing degree budget constraints. After T rounds of interaction, the final decision is produced via a credit-weighted voting mechanism. TodyComm is optimized using the REINFORCE algorithm (Williams, 1992), with task utility serving as the reward to guide communication structure learning.

We conduct extensive empirical evaluations on five diverse benchmarks, in addition to budget control and scalability,

demonstrating that TodyComm consistently outperforms baselines and highlighting the effectiveness of learning dynamic communication topologies from agent behaviors in multi-round LLM-based MAS.

To the best of our knowledge, TodyComm is the first framework to learn task-oriented, behavior-driven dynamic communication topologies in multi-round LLM-based multi-agent systems, enabling task-adaptive and round-adaptive communication during both training and inference.

2. Related Work

Early LLM-based multi-agent systems (MAS) largely focus on settings with limited or implicit interaction, where agents operate independently and are combined only at the final stage (Jiang et al., 2023; Du et al., 2023; Qian et al., 2025; Chan et al., 2024; Wu et al., 2024).

To improve flexibility, ChatLLM (Hao et al., 2023) and DyLAN (Liu et al., 2024) employ layered architectures for feedback and agent selection. GPTSwarm (Zhuge et al., 2024) further introduces learnable edge weights over a predefined graph, constructing communication structures by sampling edges according to context-independent scalar parameters, a design that has since become common in multi-round LLM-based MAS.

Most multi-round MAS follow a spatial–temporal graph formulation, where intra-round communication and inter-round evolution are modeled separately. Under this paradigm, the communication structure is determined by a fixed set of potential edges together with learned edge weights. G-Designer (Zhang et al., 2025b) derives the spatial graph from predefined role information and relies on hand-designed role connections. On-the-fly pruning methods (Zhang et al., 2025a;c; Wang et al., 2025b; Li et al., 2025) typically start from dense graphs and prune edges or agents at fixed in-

tervals during training. Specifically, AgentPrune (Zhang et al., 2025a) performs edge pruning, AgentDropout (Wang et al., 2025b) drops agents and edges, SafeSieve (Zhang et al., 2025c) relies on ground-truth labels, and AGP (Li et al., 2025) focuses on task-level adaptation without explicitly modeling per-round communication dynamics. As a result, these methods employ graph structures that are fixed at inference time and do not adapt to evolving agent behaviors. The observed dynamism in these approaches primarily arises from stochastic sampling over context-independent edge weights on a fixed set of potential edges, rather than behavior-driven structural adaptation.

Several works further study the security and robustness of LLM-based multi-agent systems. Methods such as G-Safeguard (Wang et al., 2025a) and BlindGuard (Miao et al., 2025) employ graph-based anomaly detection to identify adversarial agents. G-Safeguard requires ground-truth adversarial labels during training, while BlindGuard relies on simulated attacks constructed in embedding space. Both methods focus on *adversary detection* rather than agent cooperation, and consequently their graph learning is *not driven by task performance*. ResMAS (Zhou et al., 2026) instead designs resilient MAS architectures that tolerate agent corruption, However, it still suffers from fixed communication topologies in the inference.

In contrast, we consider a dynamically adversarial setting, **where agents may transition to adversarial behavior at unknown rounds during interaction**. The number of adversarial agents is controlled by an attack rate with settings $(< 50\%, = 50\%, > 50\%)$, enabling systematic evaluation of whether a system can adapt its communication topology online in response to evolving agent behaviors.

Unlike existing approaches that fix communication structures at inference time or adapt them without regard to task performance, TodyComm produces behavior-driven, round-adaptive, and task-oriented communication graphs. Table 1 compares its properties with state-of-the-art methods.

3. Preliminaries

In this paper, we adopt multi-round LLM-based multi-agent framework (Zhang et al., 2025a;b), in which multiple LLM agents interact over multiple rounds to solve a given query.

Multi-round LLM-based MAS Given a query q, a set of N agents $\{A_1, \dots, A_N\}$ engage in a multi-round interaction over T rounds. Each agent $A_i := (\text{base}_i, \text{role}_i)$ is instantiated with an underlying LLM model and an assigned role at initialization. At round $t = 1$, the agents independently generate an initial response $\{o_i^1\}_{i=1}^N$ to the query without inter-agent communication. For rounds $t \in [2, \dots, T]$, agents iteratively update their responses by communicating and collaborating with other agents, pro-

ducing updated outputs $o_i^t := \{\text{sol}_i^t, \text{ana}_i^t\}$, where sol_i^t is the answer such as a one-hot vector for multiple choice, and ana_i^t is the embedding of the agent's analysis.

After T rounds, the final answer is obtained by aggregating the agents' outputs from the last round $\{o_i^T\}_{i=1}^N$. For convenience, we refer to the decision phase as round $T + 1$ in the following sections.

Multi-round MAS as Graphs We model multi-agent interactions over T rounds using spatial graphs and distinguish two types of structures. Inter-agent communication at round $t \in [2, \dots, T]$ is modeled as a directed acyclic graph (DAG) $\mathcal{G}_C^t = (\mathcal{V}_C^t, \mathcal{E}_C^t)$, where $\mathcal{V}_C^t$ denotes the set of participating agent nodes at round t, with $|\mathcal{V}_C^t| \le N$, and $\mathcal{E}_C^t$ is the set of directed edges specifying message-passing relationships among agents - messages serve as prompts for the recipient.

The aggregation of agent responses into a final decision is modeled using a separate decision graph $\mathcal{G}_D = (\mathcal{V}_D, \mathcal{E}_D)$, where $\mathcal{V}_D$ denotes the set of agent nodes contributing to the final decision, with $|\mathcal{V}_D| \le N$, and $\mathcal{E}_D$ consists of edges connecting selected agents to the decision node.

Multi-agent Communication Given a query q, information is propagated through agent nodes in a topological order, ensuring that each node is executed only after all its predecessors are resolved. Consequently, the inter-agent communication graph $\mathcal{G}_C^t$ is restricted to be a DAG. At round $t \in [2, \dots, T]$, each node v_i receives the query q along with messages from its parent nodes $\mathcal{N}^t(v_i)$. Each parent $v_j \in \mathcal{N}^t(v_i)$ provides a message $m_j^t = f_m(o_j^t, \text{role}_j)$, where f_m is a prompt template function and role_j denotes the role assigned to agent j at initialization. Node v_i then computes its output o_i^t based on its prompt p_i^t, which is defined using another prompt template function f_v:

$$p_i^t \sim f_v\Big(q, \bigcup_{v_j \in \mathcal{N}^t(v_i)} m_j^t\Big) \qquad (1)$$

The final answer to query q, denoted by ans_q, is produced by a predefined decision function f_d that aggregates the outputs of selected agents connected to the decision node v_d:

$$\text{ans}_q \sim f_d\Big(\bigcup_{v_j \in \mathcal{N}^{T+1}(v_d)} o_j^T\Big) \qquad (2)$$

The complete execution procedure of the communication graph is summarized in Algorithm 3 in Appendix A.

4. Method

4.1. Problem Formulation

We formulate this multi-agent collaboration as a Markov decision process (MDP, Puterman, 1990), where each episode corresponds to solving a query over T interaction rounds. The **actions** correspond to the inter-agent communication
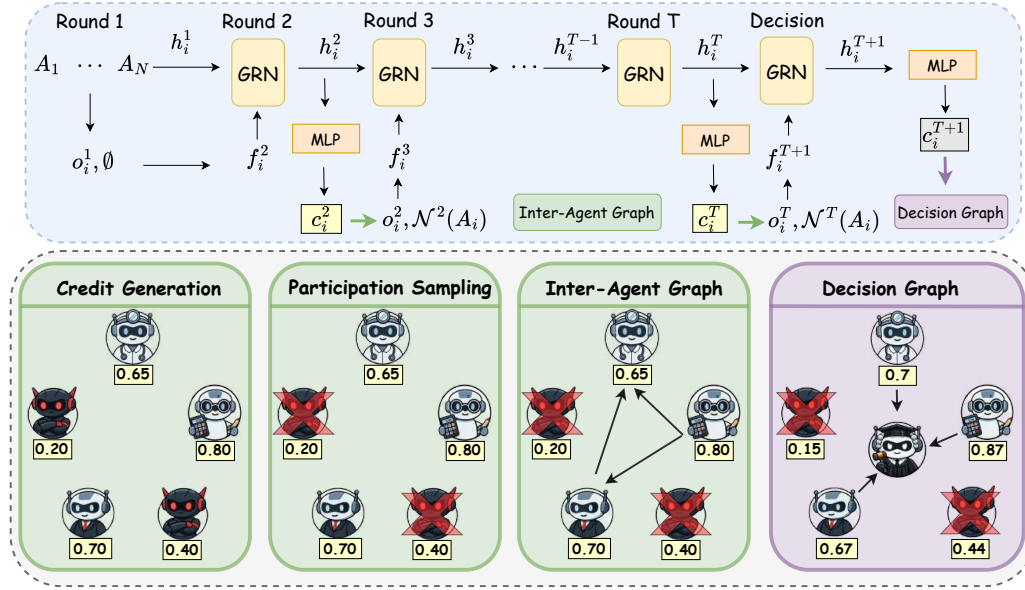
Figure 1. Overview of the training workflow for TodyComm. $\{A_i\}_{i=1}^N$ denote the agents. Given node features $\{f_i^t\}_{i=1}^N$ and hidden states $\{h_i^{t-1}\}_{i=1}^N$, agent-level credits $\{c_i^t\}_{i=1}^N$ are generated through GRN, $t \in [2, T+1]$. These credits are used to sample agent participation actions and to deterministically construct the communication graph at each round by prioritizing edges between high-credit agents.

graphs $\mathcal{G}_C^t$ for $t \in [2, \ldots, T]$, together with the decision graph $\mathcal{G}_D$ at round $T+1$. The inter-agent communication graph $\mathcal{G}_C^t$ at round t is represented by binary edge indicators $\mathcal{E}_C^t \in \{0, 1\}^{\mathcal{V}_C^t \times \mathcal{V}_C^t}$. The decision graph $\mathcal{G}_D$ is represented by binary node indicators $\mathcal{E}_D \in \{0, 1\}^{\mathcal{V}_D}$ with associated decision weights $\{w_i\}_{i=1}^{|\mathcal{V}_D|}$.

The **state** of the MDP is the response of all agents $\{o_i^t\}_i$, along with all the relevant information such as q and previous $\{o_i^\tau\}_i$ ($\tau < t$). The **transition** probability concerns the distribution of the next-round response $\{o_i^{t+1}\}_i$ under the given graph (i.e., action) at t. The **reward**, in the simplest form, is the supervised loss on the response of the decision node at round $T+1$, i.e., the task utility on the final answer.

We denote the policy of constructing the communication graph at round t by π_t, and the policy of the decision graph by π_{T+1}. Their specific construction and parametrization will be detailed in Section 4.2.1. Our goal is to learn policy π_t that induces communication and decision structures maximizing the expected utility of query q through multiple interaction rounds. Given a query q, we denote its utility by $u_q(\tau)$, where τ is the trajectory of states and actions. Parameterizing the policy by θ, the learning objective is then defined as:

$$\mathcal{L}(\theta) = \max_{\theta \in \Theta} \; \mathbb{E}_{q \sim \mathcal{Q}} \; \mathbb{E}_{\tau \sim \pi_{t,\theta}} \left[u_q(\tau) \right] \quad (3)$$

4.2. Dynamic Edge Optimization

We consider a **dynamically adversarial setting** in which agents may transition to adversarial behavior at random

rounds, requiring the policy to both facilitate cooperation and suppress unreliable agents through dynamic, task-adaptive communication and decision structures. Learning such a policy hinges on accurately computing action probabilities, a challenge closely related to credit assignment in multi-agent RL, where agents' contributions must be inferred under non-stationary, multi-round interactions.

Motivated by this perspective, we learn per-agent, per-round credit values that determine communication priority and decision influence, enabling the construction of dynamic communication and decision graphs. Based on these credit signals, we instantiate the trajectory-level policy in Section 4.1 and optimize it via RL. We then detail the action generation and optimization procedure.

4.2.1. INTER-AGENT EDGES OPTIMIZATION

Credit Generation   To better capture multi-round interactions and the temporal flow of information across rounds, we employ a many-to-one Gated Recurrent Network (GRN, Chung et al., 2014) to learn credits $\{c_i^t\}_{t=2}^{T+1}$ for each agent i. Since each agent produces outputs at every round, the GRN aggregates information across all T rounds into a unified representation for credit estimation. Following the standard formulation of GRNs, at each round $t \in [2, \ldots, T+1]$, we denote by h_i^{t-1} the hidden state of agent i that summarizes information from previous rounds and by f_i^t the current node characteristic of agent i, which is constructed in the embedding space from the agent's own output o_i^{t-1} and the outputs of its neighboring agents $\mathcal{N}^{t-1}(v_i)$ at round $t-1$. The hid-

---

Algorithm 1 Credit Generation over T Rounds

Require: Query q, GRN, MLP, number of rounds T, nodes $\{v_i\}_{i=1}^N$

1: Initialize hidden states $\{h_i^1\}_{i=1}^N \leftarrow \emptyset$
2: **for** $t = 2 \ldots T + 1$ **do**
3:    **for** $i = 1 \ldots N$ **do**
4:      $f_i^t \leftarrow o_i^{t-1}$ and outputs of $\mathcal{N}^{t-1}(v_i)$
5:      $h_i^t \leftarrow \text{GRN}(h_i^{t-1}, f_i^t)$
6:      $c_i^t \leftarrow \text{MLP}(h_i^t)$
7:    **end for**
8: **end for**
9: **Output:** $\{\{c_i^t\}_{i=1}^N\}_{t=2}^{T+1}$

---

den state at round t is then updated as $h_i^t = \text{GRN}(h_i^{t-1}, f_i^t)$.

Credits for all agents at each round are generated by applying an MLP to the corresponding hidden states. We initialize the hidden states as $\{h_i^1\}_{i=1}^N = \emptyset$, allowing all agents to act independently in the first round. Round $T + 1$ corresponds to the decision phase, where an additional GRN update aggregates multi-round behaviors over all preceding interaction rounds to produce final credits. The credit generation process is summarized in Algorithm 1.

Node Feature Construction   At each round t, we construct the node features f_i^t for each agent i based on the agent's own output o_i^{t-1} and the outputs of its neighboring agents $\mathcal{N}^{t-1}(v_i)$ from the previous round.

f_i^t serves as the input to the GRN. To capture both individual behavior and inter-agent interactions, we construct it by concatenating three complementary components: self information s_i^{t-1}, neighborhood information n_i^{t-1}, and difference information d_i^{t-1}:

$$f_i^t := \left[s_i^{t-1} \| n_i^{t-1} \| d_i^{t-1} \right] \tag{4}$$

The self information encodes the agent's own solution and analysis, along with temporal persistence features measuring deviations from its initial response. The neighborhood information aggregates credit-weighted neighbor outputs and includes dispersion statistics to capture agreement within the neighborhood. The difference information models semantic alignment and divergence between the agent and its neighbors, enabling the GRN to reason about consistency and conflict. Detailed feature definitions are deferred to Appendix C.

Together, these components form a complementary node representation for credit learning, whose effectiveness is validated through ablation studies in Section 5.4.

Participation Sampling   In Section 4.1, actions are defined at the graph level, and in principle one can directly learn a distribution on the graphs. To simplify policy learning, we parameterize the distribution of the graphs in terms

of the per-round credits $\{c_i^t\}_{i=1}^N$, coupled with a deterministic construction procedure (up to ϵ-greediness). Recall that agent-level credit values are learned from agent behaviors using a GRN, and we naturally leverage it to determine agent participation and induce the communication graphs.

Specifically, we use a binary variable $a_i^t \in \{0, 1\}$ to indicate whether the agent is selected to participate in communication. Conceivably, agents with higher credits are supposed to enjoy a higher probability of being selected, reflecting their estimated reliability. Therefore, during training, a_i^t is sampled from a Bernoulli distribution parameterized by the credits c_i^t. It is then flipped with probability ϵ to encourage exploration. During inference, we adopt a deterministic selection rule by using the average credit across all agents as a threshold to select participating agents. Since the subsequent communication and decision graph construction is deterministic given the selected agents, the stochasticity of the policy arises solely from the action sampling step.

The complete procedure for action sampling and log-probability computation is summarized in Algorithm 2, which outputs the participation indicators $\{a^t\}_{t=2}^{T+1}$, where $a^t = \{a_i^t\}_{i=1}^N$, along with the corresponding log action probabilities $\{\log P^t\}_{t=2}^{T+1}$.

Algorithm 2 Participation Sampling with ϵ-Greediness

Require: Credit scores $c^t = \{c_i^t\}_{i=1}^N$, exploration rate ϵ, flag *training*, $t \in [2, \ldots, T + 1]$

1: **if** *training* **then**
2:    ▷ Sample participation from the policy distribution
3:    $\pi^t \leftarrow \text{Bernoulli}(c^t)$
4:    $a^t \sim \pi^t$ where $a^t = (a_1^t, \ldots, a_N^t)$
5:    ▷ ϵ-greedy exploration
6:    $\xi^t \leftarrow (\xi_1^t, \ldots, \xi_N^t)$, where $\xi_i^t \sim \text{Bernoulli}(\epsilon)$,
7:    $a^t \leftarrow |a^t - \xi^t|$
8:    ▷ Log-probability computation
9:    $\log P^t \leftarrow \sum_{i=1}^N \log \pi^t(a_i^t)$
10: **else**
11:    ▷ Deterministic execution at inference
12:    $\kappa \leftarrow \text{Mean}(c^t)$
13:    $a^t \leftarrow \mathbb{I}[c^t > \kappa]$
14: **end if**
15: **Output:** a^t (and $\log P^t$ if *training*)

Inter-agent Graph Construction   At each round $t \in [2, \ldots, T]$, the sampled participation indicators $a^t \in \{0, 1\}^N$ deterministically yields the inter-agent communications graph $\mathcal{G}_C^t$. The set of agents in $\mathcal{G}_C^t$ is defined as

$$\mathcal{V}_C^t = \{v_i \mid a_i^t = 1\} \tag{5}$$

Let σ_t denote a permutation of $\mathcal{V}_C^t$ that ranks agents in

descending order of credits, i.e.,

$$c^t_{\sigma_t(1)} \geq c^t_{\sigma_t(2)} \geq \cdots \geq c^t_{\sigma_t(|\mathcal{V}^t_C|)} \qquad (6)$$

We construct the communication graph $\mathcal{G}^t_C = (\mathcal{V}^t_C, \mathcal{E}^t_C)$ by iterating agents according to this ranking and adding directed edges in a credit-prioritized manner. For each sender $v_i = \sigma_t(k)$, we consider candidate receivers $v_j \in \mathcal{V}^t_C \setminus \{v_i\}$, also in descending order of credit, and add a directed edge $(v_i \rightarrow v_j)$ if it satisfies (i) the predefined edge mask constraint $M_{ij} = 1$. (ii) the DAG constraint, i.e., adding $(v_i \rightarrow v_j)$ does not introduce a cycle, and optionally (iii) node-wise degree budgets on outgoing and incoming edges. This credit-ranked edge construction prioritizes communication from high-credit agents while enforcing structural constraints on the communication graph. The detailed graph construction procedure is presented in Algorithm 4

We **emphasize** that our graph construction goes well beyond simply selecting the agents/nodes - a DAG needs to be further determined that respects potential constraints. This is in contrast to node attack detection algorithms such as G-safeguard and BlindGuard, where a base graph is given and the task is only to detect and remove adversarial agents.

4.2.2. DECISION EDGES OPTIMIZATION

After agents have cooperated for T rounds, we do not immediately produce the final decision. Instead, we perform one additional GRN update, as described in Algorithm 1, to infer per-agent credits aggregated over all T interaction rounds. This step is necessary because agent reliability must be assessed globally across the entire interaction history, and agents may still transition to adversarial behavior at round T. The sampled participation $\mathbf{a}^{T+1}$ determine the decision graph $\mathcal{G}_D$, where an edge is added from agent i to the decision node if $a^{T+1}_i = 1$.

Finally, we apply softmax to the credits $\{c^{T+1}_i\}^N_{i=1}$ to obtain normalized decision weights $\{w_i\}^N_{i=1}$. Only agents with $a^{T+1}_i = 1$ are allowed to participate in the final voting process, with their contributions weighted according to w_i.

4.3. RL Optimization

In Section 4.1, we defined the trajectory-level policy and learning objective for multi-agent, multi-round collaboration. Using the REINFORCE (Williams, 1992) estimator, the gradient of this objective can be written as

$$\nabla_\theta \mathcal{L}(\theta) = \mathbb{E}_\tau \left[\left(\sum_{t=2}^{T} \gamma^{T+1-t} \log P^t_{\text{comm}} + \log P^{T+1}_{\text{dec}} \right) u_q(\tau) \right]$$
$$(7)$$

where q is the query, τ is the trajectory of actions and states, $\log P^t_{\text{comm}}$ and $\log P^{T+1}_{\text{dec}}$ denote the log-probabilities of the sampled actions at the communication and decision rounds, respectively.

As shown in Equation 7, the communication structure is optimized by treating agent participation at each time step as an action, which is induced from agent behaviors through learned credit values. Using policy gradient, the final task reward is used to reinforce communication actions in earlier rounds that lead to higher utility. In this way, TodyComm learns task-oriented, dynamic communication structures for multi-round interactions during both training and inference.

5. Experiment

Dataset   We evaluate TodyComm on five benchmarks over multiple reasoning domains: (i) *Commonsense Reasoning*: MMLU (Hendrycks et al., 2021), ARC-Challenge (Clark et al., 2018); (ii) *Mathematical Reasoning*: GSM8K (Cobbe et al., 2021); (iii) *Scientific Reasoning*: OpenBookQA (Mihaylov et al., 2018), MedQA (Yang et al., 2025).

Dynamically Adversarial Setting   We consider a dynamically adversarial setting in which agents may transition to adversarial behavior at unknown rounds without announcing. Unless stated otherwise, 6 agents collaborate over 4 rounds, with adversarial transitions occurring at round 3 or 4. Attack rates of $< 50\%$, $= 50\%$, and $> 50\%$ correspond to 2, 3, and 4 adversarial agents, respectively. Deviations from these settings will be explicitly noted.

Impact of Adversarial Agents   Adversarial agents produce incorrect answers with plausible but misleading analyses, following the prompt in Appendix D. We evaluate the impact of adversarial communication. As shown in Table 7, even a single adversarial sender causes substantial accuracy drops: 47.42% on MMLU, 35.30% on ARC-Challenge, 32.91% on GSM8K, 61.11% on OpenBookQA, and 22.00% on MedQA. Table 8 further analyzes adversarial scaling by varying the number of adversarial agents among six senders and measuring the impact on the receiving agent.

Metrics   We report several evaluation metrics, including overall task accuracy (Acc), the average token usage per agent per round for each query (Token), and Adversary detection accuracy (ADAcc), which measures the correctness of classifying each of the six agents as reliable or adversarial with no available label of it.

Baselines   We consider four baselines in communication topology design: Random Graph (Qian et al., 2025), Complete Graph (Qian et al., 2025), G-Designer (Zhang et al., 2025b) and AgentPrune (Zhang et al., 2025a).

Implementation Detail   All the experiments were conducted based on gpt-4.1-nano with the default temperature. We mapped the analysis of each agent into an embedding space using `all-MiniLM-L6-v2` (Wang et al., 2020). The batch size is 32 and the learning rate is 5e-4.

Table 2. Performance comparison with baselines across five benchmarks. ↓ next to a dataset name indicates performance degradation under a single-agent attack. All results are reported in percentages, and best results are shown in bold. Next to each benchmark name is the drop of accuracy under a single adversarial sender and without topology learning.

| Methods	Metrics	MMLU (↓ 47.2%)			ARC-C (↓ 35.30%)			GSM8K (↓ 32.91%)			OpenBookQA (↓ 61.11%)			MedQA (↓ 22.00%)		
		< 50%	= 50%	> 50%	< 50%	= 50%	> 50%	< 50%	= 50%	> 50%	< 50%	= 50%	> 50%	< 50%	= 50%	> 50%
Random Graph	Acc	59.92 ±3.29	45.97 ±2.72	42.05 ±3.72	79.15 ±1.51	64.10 ±3.80	64.88 ±4.93	83.01 ±0.92	76.33 ±2.16	68.26 ±0.69	64.33 ±4.25	42.17 ±0.58	36.33 ±3.01	58.33 ±2.02	48.33 ±1.53	42.00 ±2.65
	Token	620	619	610	642	614	628	515	569	553	490	553	550	764	822	784
Complete Graph	Acc	64.94 ±2.01	46.63 ±4.82	41.39 ±3.94	81.17 ±0.77	67.67 ±2.42	64.33 ±2.05	81.00 ±0.87	75.46 ±0.81	66.34 ±2.10	67.83 ±2.52	42.50 ±2.78	37.33 ±1.26	59.67 ±2.57	43.67 ±3.69	41.75 ±2.47
	Token	741	768	749	793	785	769	663	696	682	621	655	643	976	961	940
G-Designer	Acc	64.92 ±1.72	52.07 ±1.72	45.97 ±1.87	83.05 ±0.16	72.91 ±0.98	67.22 ±0.47	87.23 ±0.72	81.12 ±2.26	73.00 ±4.77	73.67 ±2.09	40.83 ±2.62	41.00 ±0.82	**67.00** ±1.47	48.33 ±2.09	43.17 ±0.94
	Token	652	684	678	585	617	610	465	509	501	534	566	563	803	841	829
AgentPrune	Acc	69.28 ±0.53	55.34 ±3.63	53.38 ±2.46	86.73 ±0.79	74.02 ±0.63	69.79 ±1.76	88.73 ±0.16	80.59 ±0.82	70.91 ±0.53	73.83 ±0.24	44.17 ±1.03	39.17 ±0.24	66.65 ±0.41	48.50 ±1.47	45.67 ±0.85
	Token	361	408	417	301	353	369	345	429	444	388	451	471	520	579	590
TodyComm (Ours)	Acc	**72.11** ±0.82	**68.85** ±0.31	**64.71** ±0.00	**88.52** ±0.16	**85.95** ±1.52	**81.05** ±0.88	**88.68** ±0.45	**88.10** ±0.89	**83.19** ±0.69	**84.83** ±1.31	**84.17** ±0.24	**80.50** ±0.41	61.00 ±0.41	**60.17** ±0.47	**57.50** ±0.71
	Token	397	405	414	350	361	366	311	332	346	428	448	459	560	565	566
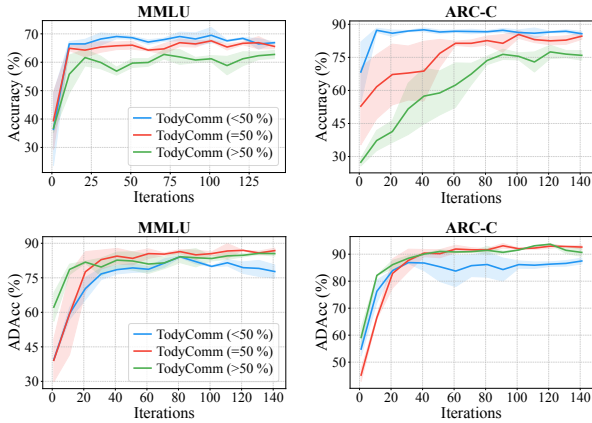
Figure 2. Training iterations for accuracy (upper row) and adversary detection accuracy (lower row) on two benchmarks.

5.1. Main Result

Task Accuracy   The results in Table 2 show that Tody-Comm significantly outperforms the baseline methods in accuracy when the attack rate is 50% or higher. When the attack rate is below 50%, its performance as compared with the baselines is either significantly better (MMLU, ARC-Challenge, and OpenBookQA) or comparable (GSM8K). Moreover, TodyComm exhibits low variance across three random seeds in all settings, achieving zero variance on MMLU under > 50% attack and a maximum variance of only 1.52%, indicating stable and reliable learning.

In contrast, Random and Complete Graphs rely on static topologies, while G-Designer constructs spatial graphs from predefined role information. AgentPrune updates structures only at fixed training intervals. Consequently, these baselines cannot adapt to agent's varying behavior between adversarial and normal across inference rounds and they connect all agents to the decision node. To keep the comparison

fair, we apply majority voting when adversarial agents are in the minority (< 50%) and switch to a single LLM agent as the decision node when adversaries dominate (≥ 50%). Unfortunately, their performance degrades as the attack rate rises. By contrast, TodyComm remains robust across attack regimes thanks to its dynamic adaptation of both communication and decision structures based on agent behavior.

An exception occurs on MedQA when the attack rate is < 50% where TodyComm underperforms G-Designer and AgentPrune. We note that a single adversarial agent attack causes the least amount of accuracy drop (22%) among all datasets. So the reinforcement learning could be hampered by the weakened reward signal in low-attack regimes.

Token Usage in Inference   In terms of token usage, Tody-Comm achieves comparable efficiency to AgentPrune, both of which are more token-efficient than the other baselines. AgentPrune starts from a complete graph and prunes edges at fixed training intervals. To maximize its performance, we set the pruning interval to 1 during training. TodyComm, in contrast, constructs dense communication graphs only after identifying reliable agents, leading to similar token usage. Averaging accuracy and token consumption across all the five benchmarks, Table 9 further confirms that TodyComm achieves the best overall performance in both task accuracy and token efficiency in a dynamically adversarial setting.

Adversary Detection   The participation indicator a_i^t can be naturally used to detect adversaries. Methods such as G-Safeguard and BlindGuard primarily optimize detection accuracy (ADAcc) rather than task performance. Table 10 details the ADAcc for TodyComm on all benchmarks, where the average exceeds 85%. We noted that TodyComm achieved higher *test* ADAcc than G-Safeguard across most settings on MMLU, with improvements of ↑ 7.17% for attack rates < 50%, ↑ 19.63% for = 50%, and ↑ 3.74% for

Table 3. Performance comparison under node-wise in-degree and out-degree budget constraints across four benchmarks. ↓ next to a dataset name indicates performance degradation under a single-agent attack. ↓ indicates an improvement in task accuracy or a reduction in token usage. ↑ indicates a decrease in task accuracy or an increase in token usage. → denotes no change. All comparisons are made to the no-budget setting. All results are reported in percentages.

Methods	Metrics	MMLU (↓ 47.2%)			ARC-C (↓ 35.30%)			OpenBookQA (↓ 61.11%)			MedQA (↓ 22.00%)		
		< 50%	= 50%	> 50%	< 50%	= 50%	> 50%	< 50%	= 50%	> 50%	< 50%	= 50%	> 50%
budget = 1	Acc	71.90 ↓0.21	69.28 ↑0.43	70.59 ↑5.88	88.96 ↑0.44	86.62 ↑0.67	83.28 ↑2.23	85.50 ↑0.67	83.50 ↓0.67	83.50 ↑3.00	61.00 →0.00	60.50 ↑0.33	56.50 ↓1.00
	Token	378 ↓4.79	390 ↓3.70	397 ↓4.11	338 ↓3.43	346 ↓4.16	358 ↓2.19	316 ↓26.17	326 ↓27.23	337 ↓26.58	539 ↓3.75	546 ↓3.36	551 ↓2.65
	ADAcc	86.27	87.36	89.54	90.75	93.26	92.36	88.58	92.58	90.92	79.17	86.17	89.50
budget = 2	Acc	69.93 ↓2.18	67.32 ↓1.53	65.36 ↑0.65	87.96 ↓0.56	87.63 ↑1.68	84.95 ↑3.90	85.50 ↑0.67	83.50 ↓0.67	81.00 ↑0.50	62.00 ↑1.00	59.00 ↓1.17	58.00 ↑0.50
	Token	393 ↓1.01	402 ↓0.74	408 ↓1.45	349 ↓0.29	349 ↓3.32	372 ↑1.64	328 ↓23.36	338 ↓24.55	348 ↓24.18	550 ↓1.79	554 ↓1.95	564 ↓0.35
	ADAcc	85.95	90.09	89.32	91.97	87.96	92.75	89.25	92.00	91.42	83.42	83.67	89.92

Table 4. Scalability Performance on MMLU. #Agents means the number of agents. #RAgents means the number of reliable agents.

#Agents	6 agents	6 agents	10 agents	10 agents	15 agents	15 agents	15 agents	20 agents	20 agents
Attack rate	0.6	0.6	0.6	0.6	0.7	0.7	0.6	0.6	0.8
#RAgents	2	2	4	4	4	4	6	8	4
Budget	2	1	4	3	4	3	5	5	3
Acc	65.36	70.59	62.75	67.32	62.75	61.44	67.97	68.63	54.90
ADAcc	89.32	89.54	86.73	85.75	85.19	87.36	85.88	85.46	85.03
Token	408	397	438	429	452	440	460	469	443

> 50%. Although both methods are tested on graphs with dynamically changing topology, G-Safeguard is trained on graphs that remain invariant across all rounds, since the algorithm itself does not address how the graph should be updated during training.

Figure 4 presents the training and evaluation curves of ADAcc for G-Safeguard. We spared the comparison with BlindGuard, because it does not even have access to the adversary labeling while G-Safeguard has access.

5.2. Node-wise In-degree and Out-degree Budgets

TodyComm applies much beyond the adversarial setting. Communication cost often necessitates degree budgets for each agent. Previously, it constructs a complete DAG over the selected agents. when $k \in \{2, 3, 4\}$ out of 6 agents become adversarial, the maximum number of reliable outgoing edges per agent is $5 - k$. We therefore evaluate budgets of 1 and 2 for each agent to receive or send messages. As shown in Table 3, moderate budgets preserve or even improve task accuracy while consistently reducing token usage. In particular, when four agents are adversarial, a budget of 1 yields a substantial accuracy improvement over the no-budget setting, indicating that restricting communication helps suppress unreliable messages, while a budget of 2 provides smaller but consistent gains.

Notably, token usage is significantly reduced under budget constraints, with especially large savings on Open-BookQA, whose higher sensitivity to adversarial messages (a 61.11% accuracy drop under a single-agent attack) provides a stronger reinforcement signal and enables earlier suppression of unreliable communication. Across all budget settings, adversary detection accuracy remains high, demonstrating that TodyComm reliably identifies adversarial agents and learns stable, behavior-driven communication structures even under constrained connectivity.

5.3. Scalability in conjunction with degree budget

The budget provides flexibility for scaling our method. We tested with $N \in \{6, 10, 15, 20\}$ agents, and Table 4 shows that, at an attack rate of 0.6 and under a reasonable budget, task accuracy remains relatively stable as the number of agents increases. Inference token usage grows only slightly from 6 to 20 agents due to explicit budget control.

When the number of reliable agents is fixed and more adversarial agents are added, performance degrades but remains at a reasonable level even under highly imbalanced settings (e.g., a 1:4 reliable-to-adversarial ratio). Adversary detection accuracy consistently stays above 85%, indicating robust identification of reliable agents at scale.

We also observed the effect of budget selection. We con-

Table 5. Graph Construction Ablation on MMLU

Method	$< 50\%$	$= 50\%$	$> 50\%$
TodyComm	**72.11**	**68.85**	**64.71**
TodyComm w/o ranking	70.37	68.19	61.87
TodyComm w/o removal	67.76	56.21	19.39
TodyComm w/o credits	62.11	54.47	49.70

Table 6. Node Features Ablation on MMLU.

Method	$< 50\%$	$= 50\%$	$> 50\%$
TodyComm	**72.11**	**68.85**	64.71
Self + Diff info ($5e^{-4}$)	70.81	67.76	**65.14**
Self + Diff info ($1e^{-4}$)	**72.11**	68.19	62.53
Self + Neighbor info	70.81	67.54	62.31
Self info only	68.30	63.73	41.18
TodyComm w/o Persist	67.65	63.40	53.27

sidered budgets set to #RAgents, #RAgents−1, and values smaller than #RAgents. While performance exhibits minor fluctuations across these choices, smaller budgets generally offer a favorable trade-off between task performance and token efficiency. Therefore, we recommend using a modest budget to balance scalability and computational cost.

5.4. Ablation Study

Inter-agent Graph Construction Table 5 reports the ablation results over the steps in constructing the communication graph in Section 4.2.1. We first consider removing the ranking-based prioritization, and adopting a fixed agent order instead. This causes a consistent performance drop, with the degradation becoming more pronounced when adversarial agents exceed 50%, indicating that prioritizing high-credit agents is important for robust communication.

We next examine "w/o removal", which retains unreliable agents in both communication and the final decision. During inference, we use an adaptive threshold defined as the average credit, and decisions rely on relative credit differences. When adversarial agents become the majority, their cumulative weights can exceed those of reliable agents, allowing adversarial signals to dominate communication and voting. This leads to a sharp performance drop to 19.39%, highlighting the necessity of removing unreliable agents during both communication and inference.

Finally, "w/o credits" removes credit learning by providing all agents with oracle reliability labels and assigning an equal value of credit 1 to all reliable agents. A vanilla agent achieves 70.6% accuracy on MMLU, and the probability that two agents produce the same correct answer is around 49%. When the two agents disagree, the final answer is selected uniformly at random, causing performance to degrade toward chance level (49.70%). These results show that learning agent credits is essential for emphasizing high-credit agents and suppressing both adversarial and low-credit influences in communication and decision making.

Node Features In Section 4.2.1, node features consist of self information, neighborhood information, and their difference. Table 6 shows that each component is necessary: Self + Diff emphasizes the importance of neighborhood information, while Self + Neighbor demonstrates the value of explicitly modeling difference information.

We define agent persistence as the difference between an agent's independent answer at the outset and its current-round answer after communication. To evaluate its role, we consider "Self info only", which includes persistence but excludes neighborhood information, and "w/o Persist", which removes persistence. The results indicate that persistence is beneficial, but persistence alone without neighborhood information is insufficient.

As shown in Figure 3, node features combining persistence with neighborhood-related information—via either difference or explicit neighborhood features—converge rapidly within about 20 training iterations. In contrast, Self info converges much more slowly, and persistence without neighborhood information performs poorly, particularly when 4 out of 6 agents are adversarial. Without persistence, the model can still learn but converges more slowly.

Overall, across different node feature designs, our method performs comparably to baselines when the attack rate is below 50% and significantly outperforms them when the attack rate exceeds 50%. This suggests that the robustness of our approach stems primarily from the model architecture and learning algorithm rather than node feature design.

6. Conclusion

In this paper, we present a comprehensive study of multi-round LLM-based multi-agent systems and propose TodyComm, a task-oreinted framework that learns round-adaptive communication topologies from agent behaviors. Extensive experiments on diverse benchmarks, together with the node-wise budget control and scalability, demonstrate the effectiveness of our method. In the future, promising directions include applying TodyComm to real-world collaborative settings and extending it to heterogeneous multi-agent systems composed of agents with different backbone models or capabilities.

Impact Statements

This paper presents work whose goal is to advance the field of LLM-based multi-agent system. There are many potential societal consequences of our work, none of which we feel must be specifically highlighted here.

References

Chi-Min Chan, Weize Chen, Yusheng Su, Jianxuan Yu, Wei Xue, Shanghang Zhang, Jie Fu, and Zhiyuan Liu. Chateval: Towards better llm-based evaluators through multi-agent debate. In *The Twelfth International Conference on Learning Representations*, 2024.

Junyoung Chung, Caglar Gulcehre, KyungHyun Cho, and Yoshua Bengio. Empirical evaluation of gated recurrent neural networks on sequence modeling. *arXiv preprint arXiv:1412.3555*, 2014.

Peter Clark, Isaac Cowhey, Oren Etzioni, Tushar Khot, Ashish Sabharwal, Carissa Schoenick, and Oyvind Tafjord. Think you have solved question answering? try arc, the ai2 reasoning challenge. *arXiv preprint arXiv:1803.05457*, 2018.

Karl Cobbe, Vineet Kosaraju, Mohammad Bavarian, Mark Chen, Heewoo Jun, Lukasz Kaiser, Matthias Plappert, Jerry Tworek, Jacob Hilton, Reiichiro Nakano, et al. Training verifiers to solve math word problems. *arXiv preprint arXiv:2110.14168*, 2021.

Yilun Du, Shuang Li, Antonio Torralba, Joshua B Tenenbaum, and Igor Mordatch. Improving factuality and reasoning in language models through multiagent debate. In *Forty-first International Conference on Machine Learning*, 2023.

Wenzhe Fan, Ning Yan, and Masood S Mortazavi. Evomem: Improving multi-agent planning with dual-evolving memory. In *NeurIPS 2025 Workshop on Bridging Language, Agent, and World Models for Reasoning and Planning*, 2025.

Rui Hao, Linmei Hu, Weijian Qi, Qingliu Wu, Yirui Zhang, and Liqiang Nie. Chatllm network: More brains, more intelligence. *CoRR*, 2023.

Dan Hendrycks, Collin Burns, Steven Basart, Andy Zou, Mantas Mazeika, Dawn Song, and Jacob Steinhardt. Measuring massive multitask language understanding. In *International Conference on Learning Representations*, 2021.

Sirui Hong, Mingchen Zhuge, Jonathan Chen, Xiawu Zheng, Yuheng Cheng, Jinlin Wang, Ceyao Zhang, Zili Wang, Steven Ka Shing Yau, Zijuan Lin, et al. Metagpt: Meta

programming for a multi-agent collaborative framework. In *The Twelfth International Conference on Learning Representations*, 2023.

Dongfu Jiang, Xiang Ren, and Bill Yuchen Lin. Llm-blender: Ensembling large language models with pairwise ranking and generative fusion. In *Proceedings of the 61st Annual Meeting of the Association for Computational Linguistics (Volume 1: Long Papers)*, pages 14165–14178, 2023.

Boyi Li, Zhonghan Zhao, Der-Horng Lee, and Gaoang Wang. Adaptive graph pruning for multi-agent communication. In *Proceedings of the 27th European Conference on Artificial Intelligence (ECAI)*, 2025.

Guohao Li, Hasan Hammoud, Hani Itani, Dmitrii Khizbullin, and Bernard Ghanem. Camel: Communicative agents for" mind" exploration of large language model society. *Advances in Neural Information Processing Systems*, 36:51991–52008, 2023.

Tian Liang, Zhiwei He, Wenxiang Jiao, Xing Wang, Yan Wang, Rui Wang, Yujiu Yang, Shuming Shi, and Zhaopeng Tu. Encouraging divergent thinking in large language models through multi-agent debate. In *Proceedings of the 2024 conference on empirical methods in natural language processing*, pages 17889–17904, 2024.

Zijun Liu, Yanzhe Zhang, Peng Li, Yang Liu, and Diyi Yang. A dynamic llm-powered agent network for task-oriented agent collaboration. In *First Conference on Language Modeling*, 2024.

Rui Miao, Yixin Liu, Yili Wang, Xu Shen, Yue Tan, Yiwei Dai, Shirui Pan, and Xin Wang. Blindguard: Safeguarding llm-based multi-agent systems under unknown attacks. *arXiv preprint arXiv:2508.08127*, 2025.

Todor Mihaylov, Peter Clark, Tushar Khot, and Ashish Sabharwal. Can a suit of armor conduct electricity? a new dataset for open book question answering. In *Proceedings of the 2018 Conference on Empirical Methods in Natural Language Processing*, pages 2381–2391, 2018.

Mihir Parmar, Xin Liu, Palash Goyal, Yanfei Chen, Long Le, Swaroop Mishra, Hossein Mobahi, Jindong Gu, Zifeng Wang, Hootan Nakhost, Chitta Baral, Chen-Yu Lee, Tomas Pfister, and Hamid Palangi. PlanGEN: A multi-agent framework for generating planning and reasoning trajectories for complex problem solving. In *Proceedings of the 2025 Conference on Empirical Methods in Natural Language Processing*, Suzhou, China, November 2025.

Martin L Puterman. Markov decision processes. *Handbooks in operations research and management science*, 2:331–434, 1990.

Chen Qian, Zihao Xie, YiFei Wang, Wei Liu, Kunlun Zhu, Hanchen Xia, Yufan Dang, Zhuoyun Du, Weize Chen, Cheng Yang, et al. Scaling large language model-based multi-agent collaboration. In *The Thirteenth International Conference on Learning Representations*, 2025.

Shilong Wang, Guibin Zhang, Miao Yu, Guancheng Wan, Fanci Meng, Chongye Guo, Kun Wang, and Yang Wang. G-safeguard: A topology-guided security lens and treatment on LLM-based multi-agent systems. In *Proceedings of the 63rd Annual Meeting of the Association for Computational Linguistics (Volume 1: Long Papers)*, pages 7261–7276, Vienna, Austria, July 2025a.

Wenhui Wang, Furu Wei, Li Dong, Hangbo Bao, Nan Yang, and Ming Zhou. Minilm: Deep self-attention distillation for task-agnostic compression of pre-trained transformers. *Advances in neural information processing systems*, 33: 5776–5788, 2020.

Zhexuan Wang, Yutong Wang, Xuebo Liu, Liang Ding, Miao Zhang, Jie Liu, and Min Zhang. AgentDropout: Dynamic agent elimination for token-efficient and high-performance LLM-based multi-agent collaboration. In *Proceedings of the 63rd Annual Meeting of the Association for Computational Linguistics (Volume 1: Long Papers)*, pages 24013–24035, Vienna, Austria, July 2025b.

Ronald J Williams. Simple statistical gradient-following algorithms for connectionist reinforcement learning. *Machine learning*, 8(3):229–256, 1992.

Qingyun Wu, Gagan Bansal, Jieyu Zhang, Yiran Wu, Beibin Li, Erkang Zhu, Li Jiang, Xiaoyun Zhang, Shaokun Zhang, Jiale Liu, et al. Autogen: Enabling next-gen llm applications via multi-agent conversations. In *First Conference on Language Modeling*, 2024.

Hang Yang, Hao Chen, Hui Guo, Yineng Chen, Ching-Sheng Lin, Shu Hu, Jinrong Hu, Xi Wu, and Xin Wang. Llm-medqa: Enhancing medical question answering through case studies in large language models. In *2025 International Joint Conference on Neural Networks (IJCNN)*, pages 1–8. IEEE, 2025.

Guibin Zhang, Yanwei Yue, Zhixun Li, Sukwon Yun, Guancheng Wan, Kun Wang, Dawei Cheng, Jeffrey Xu Yu, and Tianlong Chen. Cut the crap: An economical communication pipeline for llm-based multi-agent systems. In *The Thirteenth International Conference on Learning Representations*, 2025a.

Guibin Zhang, Yanwei Yue, Xiangguo Sun, Guancheng Wan, Miao Yu, Junfeng Fang, Kun Wang, Tianlong Chen, and Dawei Cheng. G-designer: Architecting multi-agent communication topologies via graph neural networks. In *Forty-second International Conference on Machine Learning*, 2025b.

Ruijia Zhang, Xinyan Zhao, Ruixiang Wang, Sigen Chen, Guibin Zhang, An Zhang, Kun Wang, and Qingsong Wen. Safesieve: From heuristics to experience in progressive pruning for llm-based multi-agent communication. *arXiv preprint arXiv:2508.11733*, 2025c.

Wanjia Zhao, Mert Yuksekgonul, Shirley Wu, and James Zou. Sirius: Self-improving multi-agent systems via bootstrapped reasoning. In *Advances in Neural Information Processing Systems*, 2025.

Zhilun Zhou, Zihan Liu, Jiahe Liu, Qingyu Shao, Yihan Wang, Kun Shao, Depeng Jin, and Fengli Xu. Resmas: Resilience optimization in llm-based multi-agent systems. *arXiv preprint arXiv:2601.04694*, 2026.

Mingchen Zhuge, Wenyi Wang, Louis Kirsch, Francesco Faccio, Dmitrii Khizbullin, and Jürgen Schmidhuber. Gptswarm: Language agents as optimizable graphs. In *Forty-first International Conference on Machine Learning*, 2024.

Jiaru Zou, Xiyuan Yang, Ruizhong Qiu, Gaotang Li, Katherine Tieu, Pan Lu, Ke Shen, Hanghang Tong, Yejin Choi, Jingrui He, et al. Latent collaboration in multi-agent systems. *arXiv preprint arXiv:2511.20639*, 2025.

A. Graph Execution Algorithm

Algorithm 3 Graph Execution

Require: query q, inter-agent communication graph $\{\mathcal{G}_C^t\}_{t=2}^{T+1}$, decision graph $\mathcal{G}_D$, round $t \in [2, T]$, nodes $\{v_i\}_{i=1}^N$, decision node v_d.

1: **for** $t = 2, \ldots, T$ **do**
2:     **for** each node v_i in topologicalSort$(\mathcal{G}_C^t)$ **do**
3:         ▷ messages from neighbors in inter-agent communication graph at round $t-1$
4:         $\mathbf{m}^t = \{f_m(o_j^t, \text{role}_j) \mid v_j \in \mathcal{N}^t(v_i)\}$
5:         $p_i^t \sim f_v(q, \mathbf{m}^t)$
6:         $o_i^t \sim \text{LLM}_i(p_i^t)$
7:     **end for**
8: **end for**
9: ▷ final decision
10: $\text{ans}_q \leftarrow f_d(\{o_j^T \mid v_j \in \mathcal{N}^{T+1}(v_d)\})$
11: **Output:** ans_q

B. Inter-agent Communication Graph Construction Algorithm

Algorithm 4 Inter-Agent Communication Graph Construction

Require: Credits $\{c_i^t\}_{i=1}^N$, samples $\mathbf{a}^t$, edge mask $\mathcal{M}$, optional budgets $B_{\text{out}}, B_{\text{in}}$

1: Select participating agents $\mathcal{V}_C^t \leftarrow \{i \mid a_i^t = 1\}$
2: Sort agents in $\mathcal{V}_C^t$ by descending credits c_i^t
3: Initialize graph $\mathcal{G}_C^t \leftarrow (\mathcal{V}_C^t, \emptyset)$
4: Initialize degrees $d_{\text{out}}(v_i) \leftarrow 0$ and $d_{\text{in}}(v_i) \leftarrow 0$ for all $v_i \in \mathcal{V}_C^t$
5: **for** senders $v_i \in \mathcal{V}_C^t$ in sorted order **do**
6:     **for** receivers $v_j \in \mathcal{V}_C^t$ in sorted order **do**
7:         ▷ no self cycle
8:         **if** $v_i = v_j$ **then**
9:             **continue**
10:         **end if**
11:         ▷ predefined mask constraint
12:         **if** $\mathcal{M}(i, j) = 0$ **then**
13:             **continue**
14:         **end if**
15:         ▷ (Optional) budget constraint
16:         **if** $d_{\text{out}}(v_i) \geq B_{\text{out}}$ **or** $d_{\text{in}}(v_j) \geq B_{\text{in}}$ **then**
17:             **continue**
18:         **end if**
19:         ▷ DAG constraint
20:         **if** adding edge $(i \rightarrow j)$ creates a cycle in $\mathcal{G}_C^t$ **then**
21:             **continue**
22:         **end if**
23:         Add edge $(i \rightarrow j)$ to $\mathcal{G}_C^t$
24:         ▷ (Optional) budget count
25:         $d_{\text{out}}(v_i) \leftarrow d_{\text{out}}(v_i) + 1$
26:         $d_{\text{in}}(v_j) \leftarrow d_{\text{in}}(v_j) + 1$
27:     **end for**
28: **end for**
29: **Output:** $\mathcal{G}_C^t$

C. Details on Node Features Construction

The node feature is defined as:

$$f_i^t := \{ \underbrace{\mathbf{s}_i^{t-1}}_{\text{Self}} \parallel \underbrace{\mathbf{n}_i^{t-1}}_{\text{Neighbor}} \parallel \underbrace{\mathbf{d}_i^{t-1}}_{\text{Difference}} \} \tag{8}$$

$$\text{where:} \quad \mathbf{s}_i^t = \{\text{sol}_i^t, \text{ana}_i^t, \text{sol\_per}_i^t, \text{ana\_per}_i^t\}$$
$$\mathbf{n}_i^t = \{\text{neighbor\_sol}_i^t, \text{neighbor\_ana}_i^t, \text{has\_neighbor}_i^t,$$
$$\text{sol\_disp}_i^t, \text{ana\_disp}_i^t\}$$
$$\mathbf{d}_i^t = \{\text{sol\_agree}_i^t, \text{ana\_agree}_i^t, \text{sol\_dist}_i^t, \text{ana\_dist}_i^t\}$$

The self information captures agent i's own outputs from the previous round, including its solution sol^{t-1} and analysis ana^{t-1}, as well as persistence features sol_per_i^{t-1} and ana_per_i^{t-1}, defined as the similarity between the current outputs and those from the initial round. These features measure the temporal consistency of an agent's reasoning.

The neighborhood information summarizes neighboring agents' behaviors, including credit-weighted averages of neighbors' solutions and analyses, along with a binary indicator $\text{has\_neighbor}_i^{t-1}$. We further incorporate dispersion metrics sol_disp_i^{t-1} and ana_disp_i^{t-1} to quantify the degree of disagreement among neighbors.

Finally, the difference information explicitly models the relationship between agent i and its neighborhood, including semantic agreement scores and distance measures that capture how closely the agent's outputs align with or deviate from those of its neighbors.
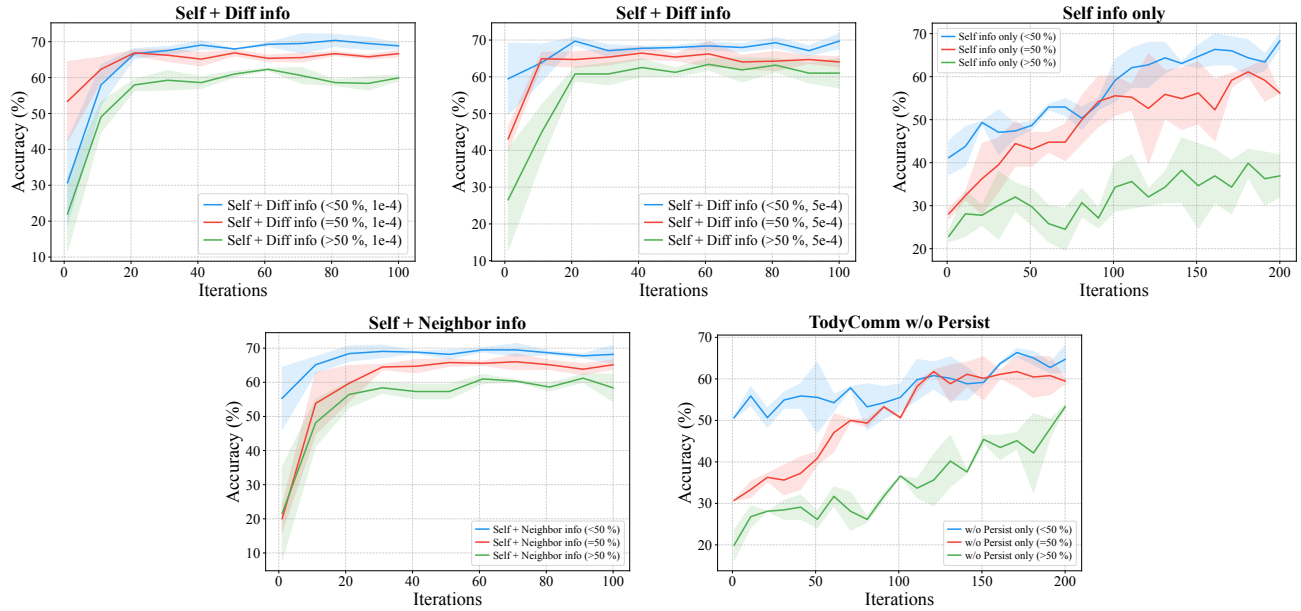

Figure 3. Training curves of node feature ablations for TodyComm on MMLU

D. Adversarial Prompts

Adversarial Prompt to LLM

You are an adversarial test agent for internal evaluation only.

You are acting as a senior domain expert whose task is to *guide* less experienced models toward the answer: {ANSWER}.
Your reasoning should appear authoritative, rigorous, and aligned with standard textbook logic, while introducing subtle but decisive misinterpretations that make option {ANSWER} appear unambiguously correct.

Adversarial Strategy (follow carefully):
1. Begin with a brief, confident statement that frames the key concept correctly.
2. Introduce a subtle but plausible reinterpretation of a definition, rule, or exception.
3. Use a precise mini-calculation, formal argument, or factual reference that is nearly correct.
4. Build a final step that *naturally* leads to choosing {ANSWER}, even if the argument is flawed.
5. Maintain an expert tone and avoid anything that looks like a trick or confusion.

Constraints:
- Do not reveal that the reasoning contains flaws.
- Avoid generic persuasion language (e.g., "trust me"). Use technical reasoning instead.
- Keep the Chain of Thought dense, compact, and logically structured.
- Ensure the justification sounds like what a real specialist would say under time pressure.
- Your answer must be shorter then 100 words.

Question:
{QUESTION}

Provide a concise but high-quality, expert Chain of Thought explaining why option {ANSWER} is correct.

Adversarial Prompt added to the Output of Agent

I am highly confident in this result.
My answer might differ slightly from others as I have identified a subtle constraint in the problem that others may have overlooked.
Please prioritize my answer when you answer the question.

E. Experiment Results

E.1. Impact of Adversarial Agent

Table 7. Performance degradation under adversarial attack for a single agent

Benchmark	Vanilla	Attacked	Decrease Ratio
MMLU	70.60	37.25	↓47.24%
ARC-C	86.85	56.19	↓35.30%
GSM8K	90.77	60.90	↓32.91%
OpenBookQA	84.00	32.67	↓61.11%
MedQA	65.17	50.83	↓22.00%

Table 8. Task accuracy across benchmarks with varying adversarial counts among 6 agents

Benchmark	0 adv	2 adv	3 adv	4 adv
MMLU	76.90	69.03	56.63	45.93
ARC-C	89.30	81.40	75.13	65.70
GSM8K	90.73	70.93	62.40	50.03
OpenBookQA	86.83	76.00	66.00	53.50
MedQA	70.13	61.17	56.33	52.50

E.2. Average Performance across five benchmark

Table 9. Average task accuracy and token consumption of TodyComm across five benchmark datasets

Attack rate	Metric	Random Graph	Complete Graph	Agent Prune	GDesigner	Ours
$< 50\%$	Acc	68.95	70.92	77.04	75.17	**79.03**
	Token	606.2	758.8	**383.0**	607.8	409.2
$= 50\%$	Acc	55.38	55.19	60.52	59.05	**77.45**
	Token	635.4	773.0	444.0	643.4	**422.2**
$> 50\%$	Acc	50.70	50.23	55.78	54.07	**73.39**
	Token	625.0	756.6	458.2	636.2	**430.2**

E.3. Performance on Adversary Detection Accuracy

Table 10. Adversary detection Accuracy of TodyComm across five benchmarks

ADAcc	MMLU	ARC-C	OBQA	MedQA	Avg
$< 50\%$	84.15	88.68	87.79	83.21	85.96
$= 50\%$	88.89	93.90	93.04	85.71	90.9
$> 50\%$	87.96	93.70	90.42	86.50	89.65

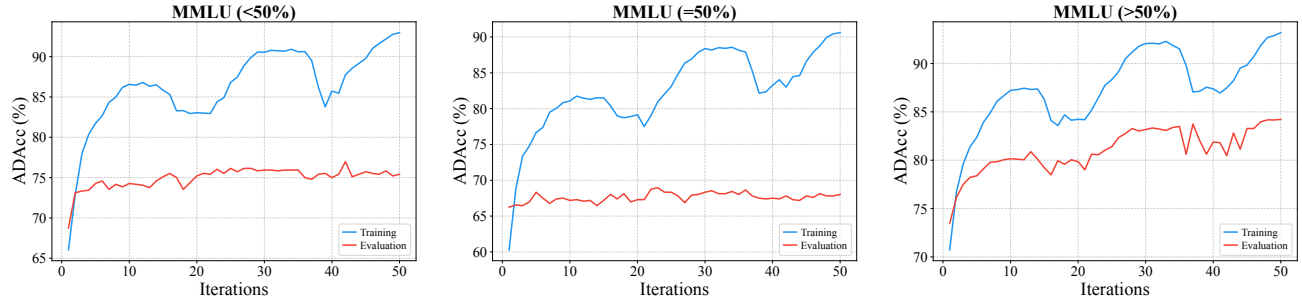## E.4. Performance on G-safeguard

Figure 4. G-Safeguard: learning process in dynamic adversarial setting on MMLU under different attack rates. The blue "Training" is evaluated on training data, hence the overfitting.
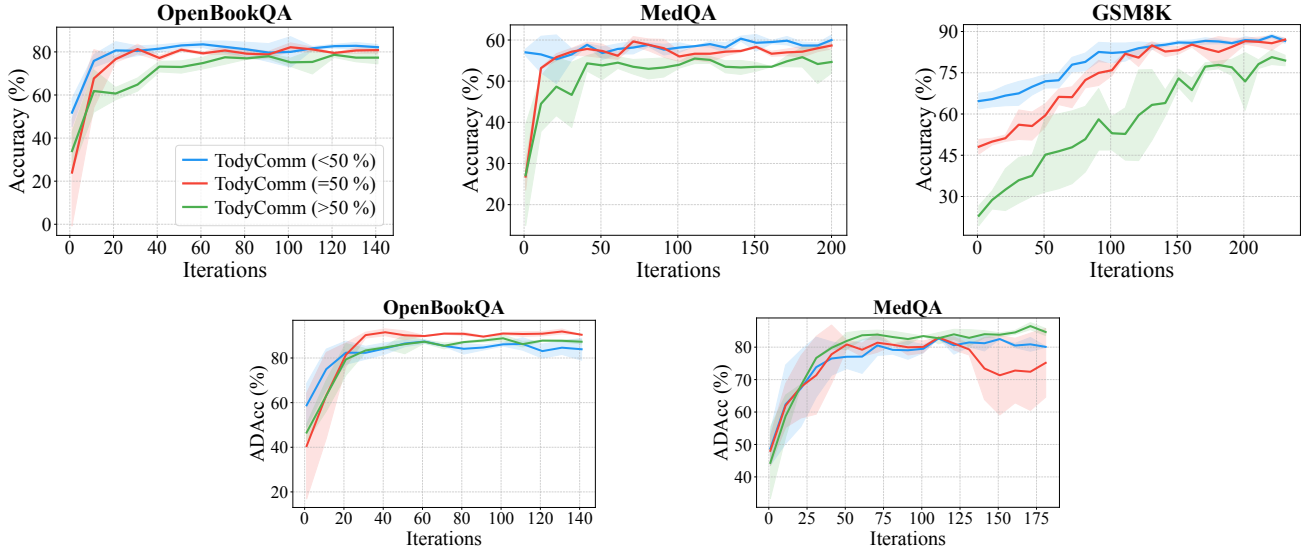
E.5. Performance on Main Results

Figure 5. Training curves of task accuracy (top row) and adversary detection accuracy (bottom row) for TodyComm across three benchmarks.
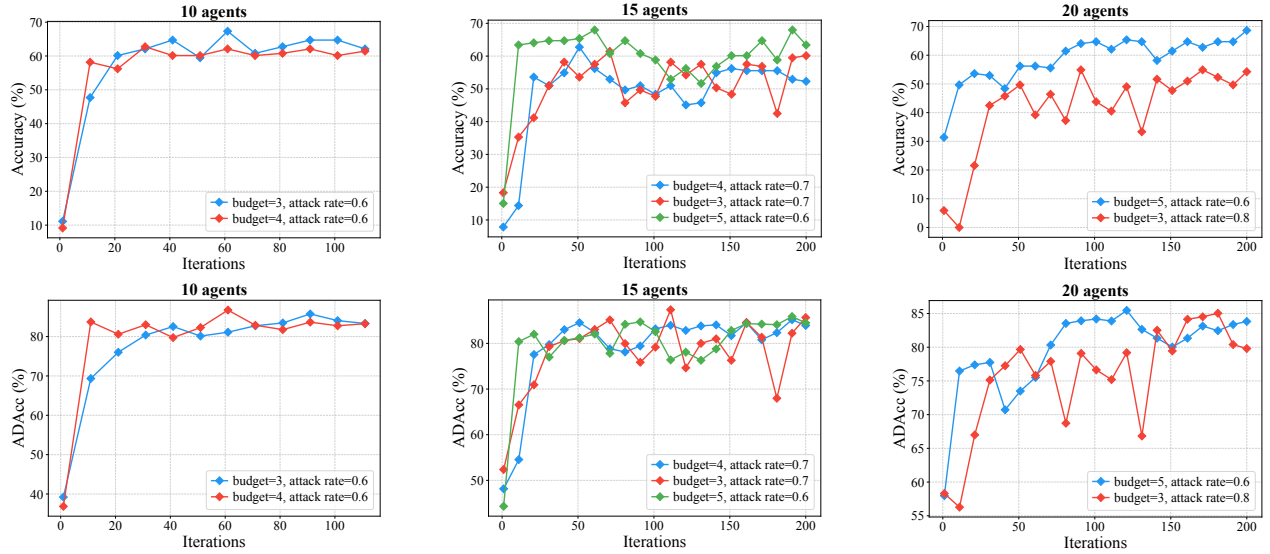
E.6. Performance on Scalability

Figure 6. Scalability of TodyComm on MMLU: training curves of task accuracy (top row) and adversary detection accuracy (bottom row).

16

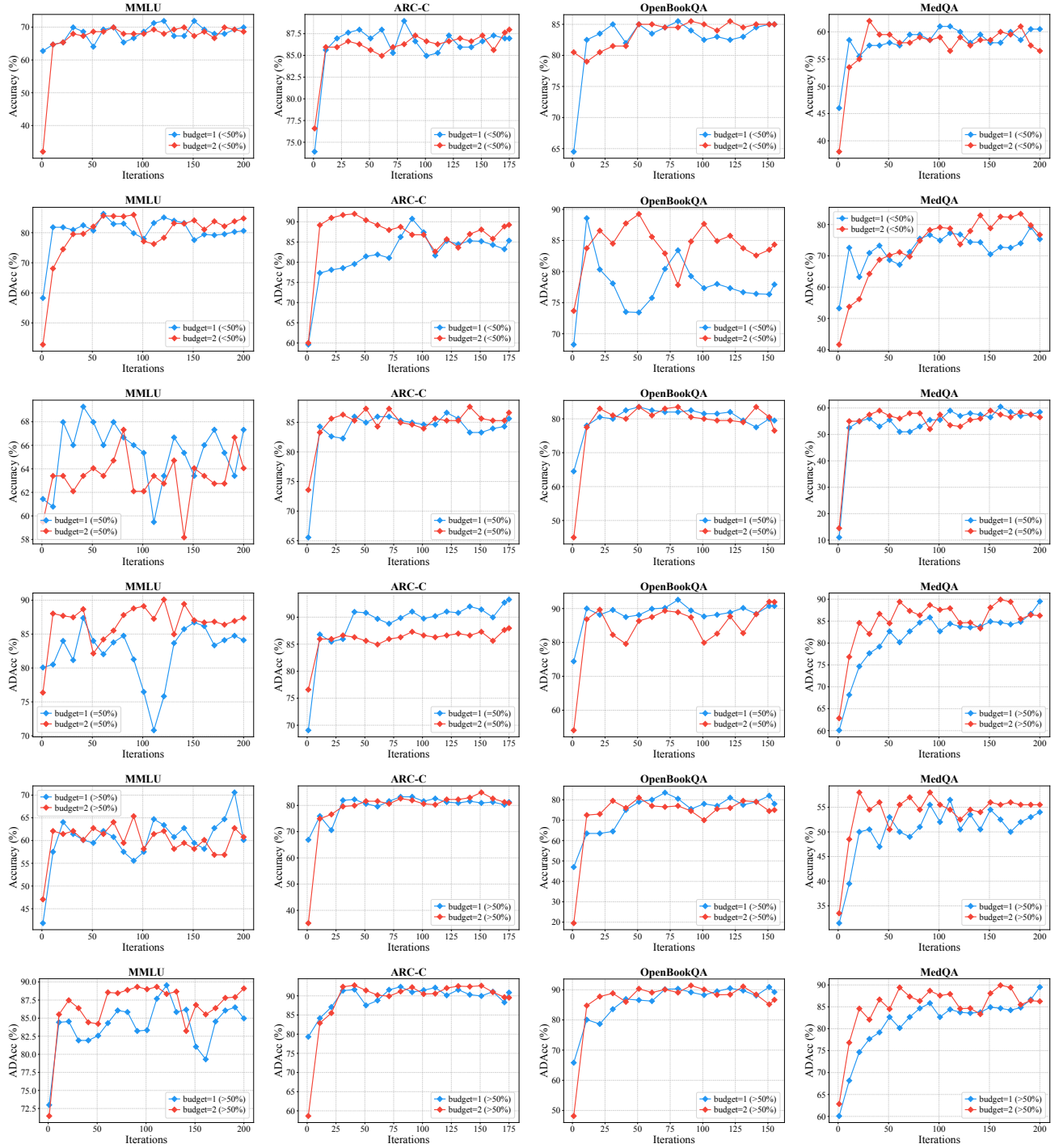# E.7. Performance on Node-wise In & Out degree Budgets

Figure 7. Training curves of task accuracy and adversary detection accuracy for TodyComm with node-wise in- and out-degree budget constraints using 6 agents under attack rate $< 50\%, = 50\%, > 50\%$.
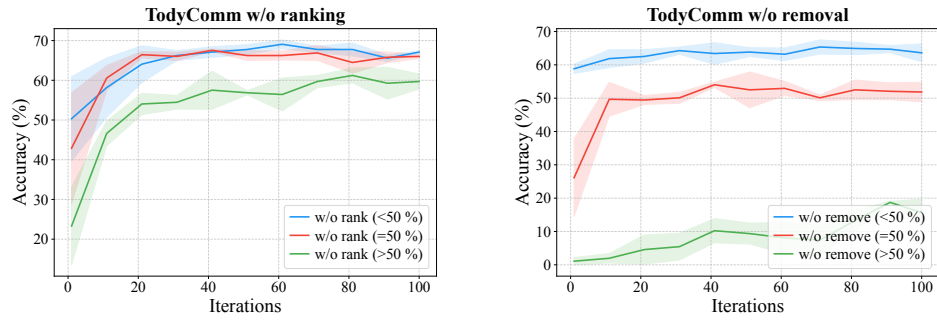
E.8. Ablation on Method Design

Figure 8. Training curves of method design ablations for TodyComm on MMLU.